Available online at www.sciencedirect.com
SCIENCE DIRECT
ELSEVIER
Journal of Crystal Growth 288 (2006) 123–127
JOURNAL OF CRYSTAL GROWTH
www.elsevier.com/locate/jcrysgro

Influence of film growth conditions on carrier mobility of hot wall epitaxially grown fullerene based transistors

A. Montaigne Ramil[a], Th.B. Singh[b,*], N.T. Haber[c], N. Marjanović[b], S. Günes[b], A. Andreev[d], G.J. Matt[b], R. Resel[c], H. Sitter[a], S. Sariciftci[b]

[a]*Institute of Semiconductor and Solid State Physics, Johannes Kepler University Linz, A-4040, Linz, Austria*
[b]*Linz Institute of Organic Solar Cells(LIOS), Physical Chemistry, Johannes Kepler University Linz, Altenbergerstrasse 69, A- 4040, Linz, Austria*
[c]*Institute of Solid State Physics, Graz University of Technology, A-8010 Graz, Austria*
[d]*Institute for Physics, University Leoben, A-8700 Leoben, Austria*

Abstract

Hot wall epitaxially grown C_{60} based organic field-effect transistors (OFETs) show relatively high electron mobilities of 0.4–1 cm^2/Vs. We report results of thin film grown with various growth conditions such as preheating and initial substrate temperatures resulting in strikingly different fullerene film nanomorphology. The mobility is enhanced up to 3 cm^2/Vs for films grown at a substrate temperatures of 130 °C. This improvement in the mobility is explained in terms of a transition from a disordered interface consisting of small-elongated grains to a well-ordered C_{60} film with bigger and rounder grains.
© 2005 Elsevier B.V. All rights reserved.

Keywords: A1. Morphology; A3. C_{60} thin film; A3. Hot wall epitaxy; B2. Organic field-effect transistors

1. Introduction

Highest reported and reproduced charge carrier mobilities obtained in organic field-effect transistors (OFETs) is 15 cm^2/Vs for rubrene single crystals [1] and in the range of 1–2 cm^2/Vs for the case of vacuum evaporated pentacene thin-films [2]. Efforts to increase the charge carrier mobility in OFETs with n-type organic materials have been difficult due to several physical reasons: (i) rapid degradation under ambient condition, (ii) electron transport properties are sensitive to impurities in the crystal [3] and (iii) difficulty with synthesizing materials having electron affinities that allow the injection of electrons from stable electrodes in air. The majority of OFETs with n-type semiconductors were fabricated based on vacuum evaporated films [4–8]. Most of these devices were grown on inorganic SiO_2 or Al_2O_3 dielectrics except for a very few grown on organic dielectrics [9]. Because of the very different physical nature of these two media, the deposition may result in highly disordered films, leading to a poor OFET performance [10]. Although the van der Waals type interactions between organic molecules and inorganic substrates are rather weak, the crystallographic phases, the orientation, and the morphology of the resulting organic semiconductor film critically depends on the interface properties and growth kinetics. In turn, the field-effect mobility is largely determined by the morphology of the semiconductor film at the interface with the gate dielectric [11]. We have considered such interface related phenomena with an attempt by growing organic semiconductor layers on top of an organic insulator and by studying their structure-performance relationship. In this paper, we present results on OFETs based on C_{60} films grown on top of organic dielectrics by hot wall epitaxy (HWE). A good interfacial organisation of the resulting C_{60} film and corresponding improvement in the mobilities of the OFETs from 0.5 to 3 cm^2/Vs are obtained by optimizing the substrate temperature during C_{60} deposition.

*Corresponding author. Tel.: +43 732 2468 8767; fax: +43 732 2468 8770.
E-mail address: birendra.singh@jku.at (T.B. Singh).

0022-0248/$ - see front matter © 2005 Elsevier B.V. All rights reserved.
doi:10.1016/j.jcrysgro.2005.12.061

2. Experimental procedure

The fabrication procedure of C_{60} OFETs is described previously [9]. Fig. 1 shows a scheme of the devices presented here and the molecular structure of the C_{60} and organic gate dielectric divinyltetramethyldisiloxane-bis(benzocyclobutane) (BCB), respectively. The C_{60} films were deposited by HWE on top of the BCB layers at a constant growth rate of 0.8 Å/s and at a residual pressure of 8×10^{-6} mbar. The working principles of a HWE system can be found elsewhere [12]. Since in all experiments reported here the film growth rate is constant, henceforth we refer only to the time of deposition instead of the physical thickness of the C_{60} layer. As schematically shown in Fig. 2 we classify two types of growth processes: (a) BCB dielectric is preheated at 250 °C for 20 min and cooled down to 130 °C or room temperature (RT) followed by the growth of the C_{60} layer at 130 °C or RT; (b) BCB dielectric is not-preheated but only warmed up to growth temperature followed by the deposition of the C_{60} layer at a substrate temperature of 130 °C or the growth started at RT. For our HWE, once the substrate is placed on top of the growth reactor it is indirectly heated through the thermal radiation emitted from the heaters of the source and wall of the C_{60} source quartz tube. This additional but not controlled amount of heat lead to a lowest reachable substrate temperature in the range of 90–100 °C. Thus it was decided to switch on the substrate heater of the C_{60} source and set it to 130 °C during the deposition of all thick C_{60} layers presented in this work. In that way we get a more controllable temperature of the substrate T_s. Device fabrication is completed by evaporation of source-drain electrode (Li/Al 0.6/60 nm) through a shadow mask under a residual pressure of 2×10^{-6} mbar. The obtained channel has a length and width of 20–25 μm and 1.4 mm, respectively. The device characterization was done using an Agilent E5273A which has one high power source-measure unit (SMU) and one with low power SMU. Atomic force microscopy (AFM) images were obtained using a Digital Instrument Dimension 3100 microscope working in tapping mode. The structural characterization of the samples was done by means of ex-situ X-ray diffraction measurement. X-ray $\omega/2\theta$ scans carried out using the CuK_α radiation with a wavelength of $\lambda = 1.54$ Å by a Siemens D501 Crystalloflex powder X-ray diffractometer.

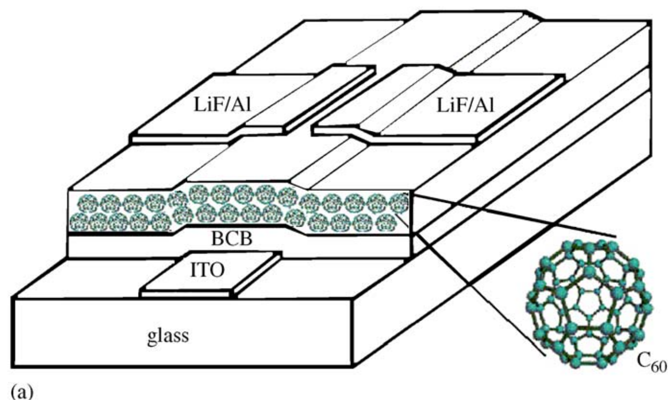

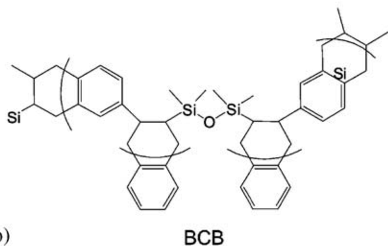

Fig. 1. (a) Scheme of the n-type C_{60} field effect transistor. The inset shows a view of a C_{60} molecule. (b) Chemical representation of divinyltetramethyldisiloxane-bis(benzocyclobutene), BCB.

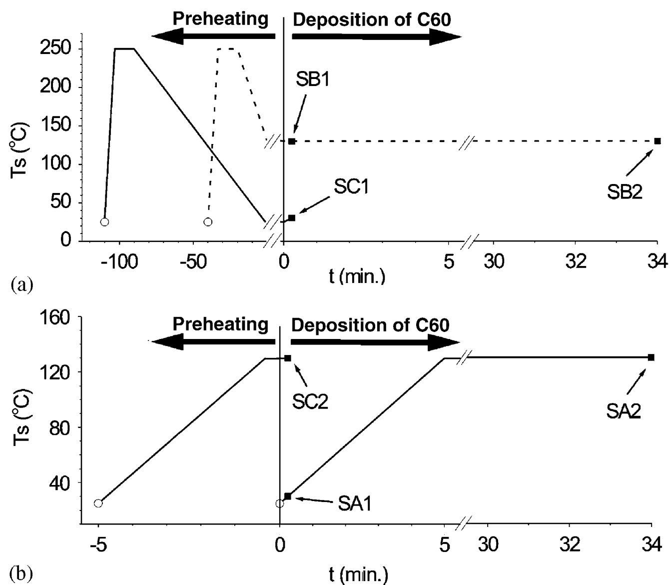

Fig. 2. Substrate temperature (T_s) vs. time (t) for the whole growth process of the C_{60} layers on BCB dielectric layers. (a) All pre-heated samples: SC1: BCB substrate is preheated and cooled down to RT and short deposit of C_{60} for 15 s. SB1: BCB substrate is preheated and cooled down to 130 °C and short deposit of C_{60} for 15 s. SB2: BCB substrate is preheated and cooled down to 130 °C and deposit the C_{60} for 34 min. (b) All no-preheated samples: SC2: BCB substrate is warmed up to 130 °C and short deposit of C_{60} for 15 s. SA1: C_{60} is deposited for 15 s and T_s is gradually increased from RT to 40 °C. SA2: C_{60} is deposited for 34 min T_s gradually reached 130 °C in the first 5 min and was kept constant at 130 °C during the rest of the growth.

3. Results and discussion

As mentioned in the introduction, FET measurements show that the first few monolayers at the interface to the dielectric layer dominate the charge transport. Therefore we will first discuss our effort to correlate the film morphology at the organic insulator/semiconductor interface with its transport properties. Comparative study of thin-film morphology with different growth condition is shown Fig. 3. Fig. 3(a) shows AFM image of C_{60} layer (sample: SA1) deposited on BCB dielectric at T_s very close

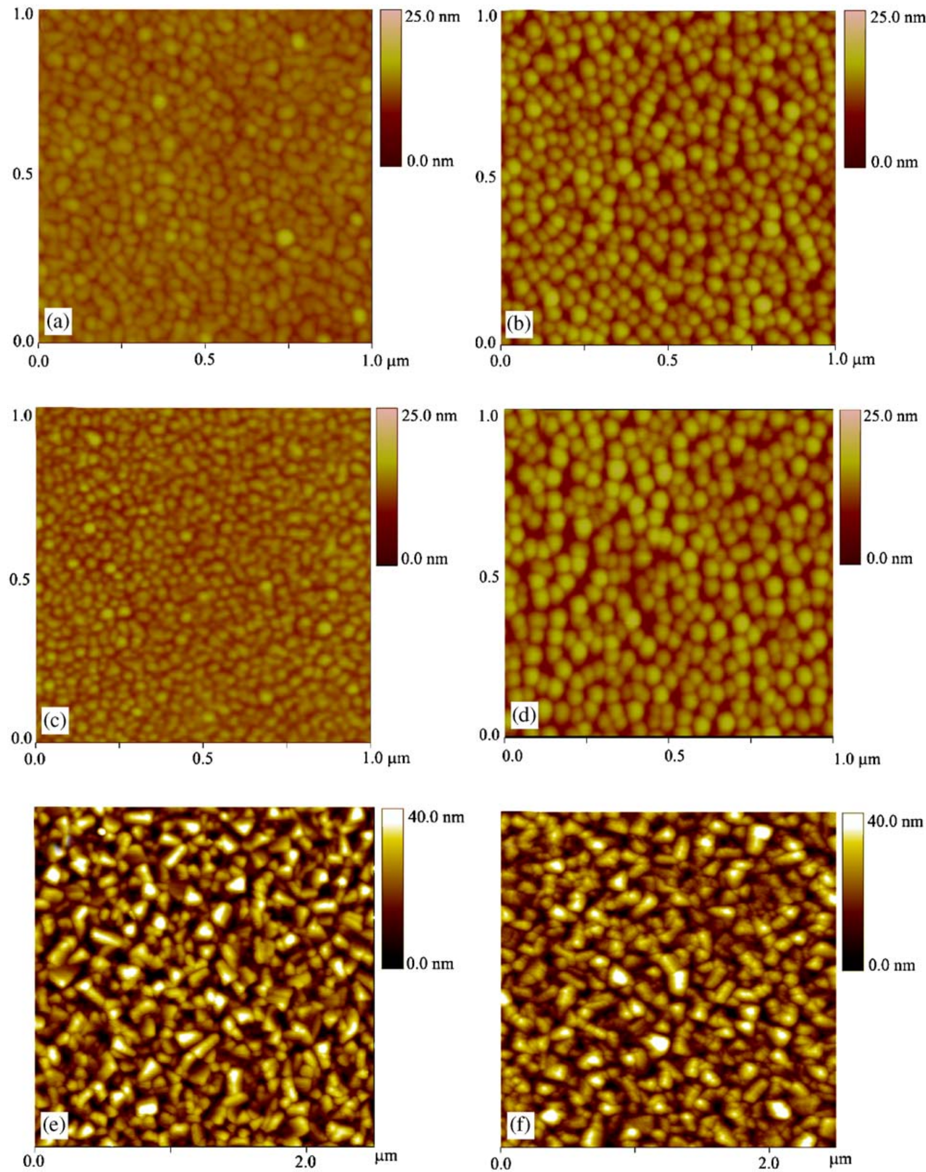

Fig. 3. AFM images of C_{60} thin films deposited on BCB dielectric. (a) SA1, (b) SB1, (c) SC1, (d) SC2, (e) SA2 and (f) SB2.

to RT (see Fig. 2(b)). In this case, elongated grains are observed with an areal density of crystallites around 500 crystallites/μm^2. When the C_{60} layer is grown on the BCB substrate once preheated at 250 °C for 20 min and cooled down to T_s of 130 °C (sample: SB1), the resulting film has a strikingly different nanomorphology as compared to SA1 in Fig. 3(b). In the latter case, a bigger grain size, a density of crystallites around 370 crystallites/μm^2 and more round granules are observed.

In order to clarify whether the observed morphological difference is due to different T_s or due to the effect of preheating of the BCB substrate, the following experiments are done. In the first case (sample: SC1), BCB substrate is preheated at 250 °C for 20 min.and cooled down to RT and subsequent C_{60} layer is grown (See Fig. 2(a)). In the second case, (Sample: SC2), BCB is heated till 130 °C and subsequently C_{60} layer is deposited (see Fig. 2(b)). The resulting AFM images of the two cases are also strikingly different as shown in Figs. 3(c) and (d). SC2 is found to be with similar features as SB1. On the other hand, the SC1 features look similar to SA1. From these morphological study, it can be concluded that the growth temperature is the dominant parameter to obtain bigger crystallites at the interface, while the preheating of the BCB seems to be not so important. However, the AFM images of preheated and not preheated BCB show in both cases a very flat surface with a roughness of less than 5 nm. Since the fabrication of C_{60} OFETs [9] involves longer growth (34 min) of C_{60} film, we will compare the surface morphology of such films (SA2 and SB2). In both cases, the resulting films show similar morphologies. That means that the surface morphology of thick films is not influenced by the morphology at the interface, since most of the growth occurs at $T_s = 130$ °C.

Our X-ray studies on SA1, SB1, SC1 and SC2 do not reveal any characteristic features mostly due to insufficient thickness of the film. Results on SA2 and SB2 have features as shown in Fig. 4. Figs. 4(a) and (b) shows C_{60} peaks of the X-ray measurements in the $\omega/2\theta$ scan mode for SA2 and SB2, respectively. The vertical dotted and dashed lines represent the theoretical values of the peak positions simulated with the software Powder Cell 2.3 for the C_{60} and ITO crystals, respectively. The graphs show a very good agreement between the simulated and the experimentally obtained peak positions. The simultaneous presence of the C_{60} peaks (1 1 1) and (2 2 0) in the X-ray patterns shows that these films are polycrystalline and the C_{60} crystallites are randomly oriented. The two amorphous components, namely the BCB dielectric and the glass, show broad halos covering the ranges of the angles 2θ from 10 to 20° and from 15° to 40°. Basically, both films have very similar positions as well as intensity and width of the C_{60} peaks which means that both films have very much alike crystalline structure. We have also observed that there is no significant difference between the X-ray patterns of the not preheated and preheated glass/ITO/BCB substrates.

The effect of the substrate temperature on initial stage of the C_{60} film growth is also reflected in the performance of the OFETs. Fig. 5 shows the square root of the source-drain current $\sqrt{I_{ds}}$ vs. $(V_{gs}-V_t)$ for drain-source voltage, $V_{ds}=60\,V$, where V_{gs} and V_t are the gate and onset voltages, respectively. The field effect mobilities μ_e obtained from these two set of devices are 0.5 and 3 cm^2/Vs for SA2 and SB2, respectively. We used here standard transistor Eq. (1) to evaluate the mobility [13]:

$$I_{ds} = \frac{\mu W C_i}{2L}(V_{gs} - V_t)^2, \tag{1}$$

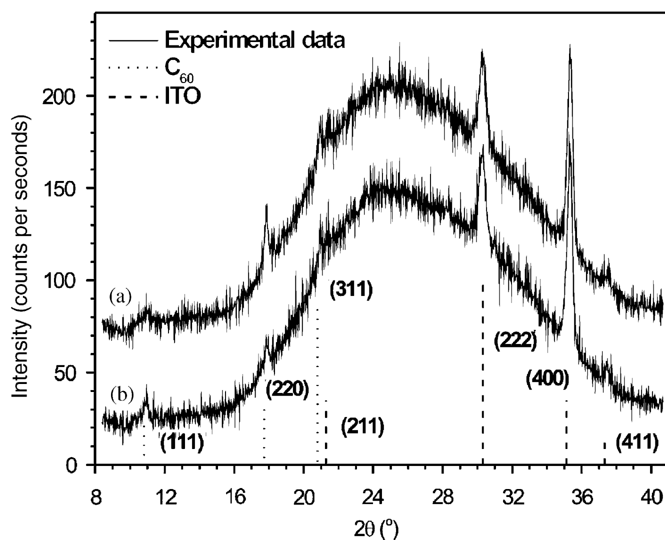

Fig. 4. X-ray $\omega/2\theta$ scan patterns for: (a) 300 nm thick C_{60} layer grown on un-preheated BCB, (b) 300 nm thick C_{60} layer grown on BCB preheated at 250 °C for 20 min. Curve (b) have been shifted down in intensity for clarity. The vertical dotted and dashed lines mark the computer simulated peak positions of C_{60} and ITO, respectively.

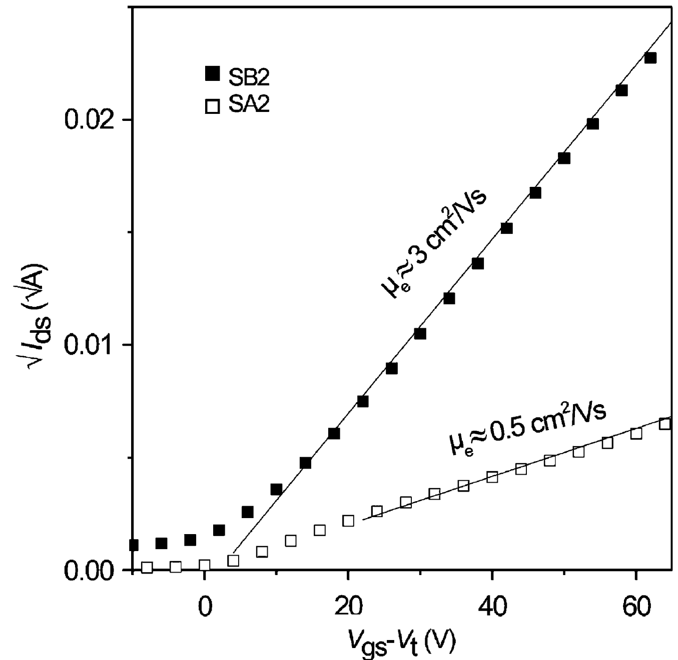

Fig. 5. $\sqrt{I_{ds}}$ vs. $(V_{gs}-V_t)$ plot for SB2 and SA2 with corresponding obtained mobility of 3 and 0.5 cm^2/Vs, respectively. The lines are theoretical fits to the experimental data using Eq. (1).

where W is the channel width, L the channel length and C_i the dielectric capacitance. In the estimation of the field-effect mobility, we have assumed a V_{gs} independent mobility and also we have not taken into account contact resistances for simplicity. The improvement in the μ_e is assumed to be due to transition of C_{60} film morphology at the interface from small elongated grains to bigger rounder and closely packed grains as depicted in Figs. 3(a) and (b).

4. Conclusions

Our results show that the temperature of the BCB dielectric during the deposition of the first few layers of C_{60} plays a crucial role in determining the better morphology of the C_{60} film at the interface and hence in the performance of the OFET. From the experimental observation, substrate pre-heating temperature is less relevant to the film morphology and hence to the device performance. An improvement in the field-effect mobility from 0.5 to 3 cm^2/Vs is observed when the temperature of the substrate is increased from nominally RT to 130 °C.

Acknowledgment

One of the authors (Th. B. S.) acknowledge the financial support of the Austrian Foundation for the Advancement of Science (FWF NANORAC Contract no. N00103000).

References

[1] V.C. Sundar, J. Zaumseil, V. Podzorov, E. Menard, R.L. Willett, T. Someya, M.E. Gershenson, J.A. Rogers, Science 303 (2004) 1644.

[2] Y.-Y. Lin, D.J. Gundlach, S.F. Nelson, T.N. Jackson, IEEE Electron Dev. Lett. 18 (1997) 606.
[3] R.G. Kepler, Phys. Rev. 119 (1960) 1226.
[4] Z. Bao, A.J. Lovinger, J. Brown, J. Am. Chem. Soc. 120 (1998) 207.
[5] H.E. Katz, J. Johnson, A.J. Lovinger, W. Li, J. Am. Chem. Soc. 122 (2000) 7787.
[6] R.J. Chesterfield, J.C. McKeen, Ch.R. Newman, C.D. Frisbie, P.C. Ewbank, K.R. Mann, L.L. Miller, J. Appl. Phys. 95 (2004) 6396.
[7] P.R.L. Malenfant, C.D. Dimitrakopoulos, J.D. Gelorme, L.L. Kosbar, T.O. Graham, Appl. Phys. Lett. 80 (2002) 2517.
[8] S. Kobayashi, T. Takenobu, S. Mori, A. Fujiwara, Y. Iwasa, Appl. Phys. Lett. 82 (2003) 4581.
[9] Th.B. Singh, N. Marjanović, G.J. Matt, S. Günes, N.S. Sariciftci, A. Montaigne Ramil, A. Andreev, H. Sitter, R. Schwödiauer, S. Bauer, Org. Electron. 6 (2005) 105.
[10] G. Horowitz, Ph. Lang, M. Mottaghi, H. Aubin, Adv. Funct. Mater. 1069 (2004) 14.
[11] F. Dinelli, M. Murgia, P. Levy, M. Cavallini, F. Biscarini, D.M. de Leeuw, Phys. Rev. Lett. 92 (2004) 116802.
[12] (a) A. Lopez-Otero, Thin Solid Films 3 (1978) 49;
(b) A. Andreev, G. Matt, C.J. Brabec, H. Sitter, D. Badt, H. Seyringer, N.S. Sariciftci, Adv. Mater. 12 (2000) 629.
[13] S.M. Sze, Physics of Semiconductor Devices, Wiley, New York, 1981.